Int. J. Multiphase Flow Vol. 6, pp. 411–423
Pergamon/Elsevier, 1980. - Printed in Great Britain

THE MECHANISM OF AIR BUBBLE ENTRAINMENT IN SELF-AERATED FLOW

P. VOLKART
Laboratory of Hydraulics, Hydrology and Glaciology annexed to the Federal Institute of Technology, Zurich, Switzerland

(*Received* 10 *October* 1979; *in revised form* 18 *February* 1980)

Abstract—The mechanism by which air bubbles are brought into a quick moving waterflow with free surface was studied. The processes taking place at the surface were visualized with a stroboscope. It shows, how the bubbles are generated by falling drops. The height of fall and the velocity with which a water drop must hit the surface in order to form an air bubble can be calculated by an energy balance. Measurements of diameter, height of fall and velocity of the drops as well as of the size of the bubbles coincide well with the obtained formulae. Results are valid for pure water and slightly dirty waste water. Such flows occur in steep smooth channels, spillways and strongly inclined partially filled conduits and pipelines.

1. INTRODUCTION

The present article deals with two-phase flow of clear or waste water and air bubbles. Such a flow happens for example in a steep and open water channel or in a spillway of a dam. But it can also occur in a strongly inclined sewer pipe or industrial pipeline. In the case of pipes it must be assumed that the conduit is only partially filled, therefore, a zone which contains mainly air and single water drops must exist above the flowing mixture of water and air bubbles. Figure 1 shows schematically the specified type of flow. Following a reservoir or an increasing slope the water which still does not contain any air bubbles becomes accelerated, due to the effect of gravity. The turbulent boundary layer $\delta(X)$ approaches the water surface and reaches it at point P_D. After an additional stretch X_σ the air bubble entrainment starts in point P_A. Finally, in point P_E a state of equilibrium is reached. Thereafter the depth of the mixture h_E remains constant. The present article deals exclusively with the process and mechanism of the air bubble entrainment downstream of point P_A.

Ehrenberger dealt for the first time (1926) with the phenomenon of natural air entrainment in steep channels with open tops. Lane (1939) observed how air bubbles can form at the crest spillway of dams by water drops plunging in. From Hickox (1945) comes the model-idea, that the air bubble entrainment starts at the point, where the so-called turbulent marginal layer reaches the water surface. At least for an approximation this hypothesis is still valid today. But the question whether the air bubbles come into the flow by water drops dipping in (Viparelli 1953, Killen 1969) or as a result of striking vortices and rollers on the surface (Frankovic 1953) still remains unanswered. Therefore, the aim of the study was to make the entrainment mechanism as visible as possible, to indicate the size and distribution of the air bubbles, and to evaluate the difference of the process in open channels vs partially filled pipelines.

2. EXPERIMENTAL EQUIPMENT

The processes taking place at the surface of the flowing mixture were made visible in a pipeline, inclined by about 12 degrees, by means of the stroboscope technique. The pipeline's length was 50 m, consisting of smooth synthetic material with an interior diameter of 240 mm. Along its length it was cut open at several points. The stroboscope consisted of an electronic flash, whose frequency could be continuously adjusted up to 350 flashes/sec and a camera with normal exposure time of 1/10–1/2 sec. Thus it was possible to expose on one picture several motion phases. Hence, one photo shows several consecutive phases of the same process, e.g. a moving water drop. Only the motion above the mixture's surface can be visualized by the stroboscope. In order to estimate the size of the air bubbles, the same instruments which were

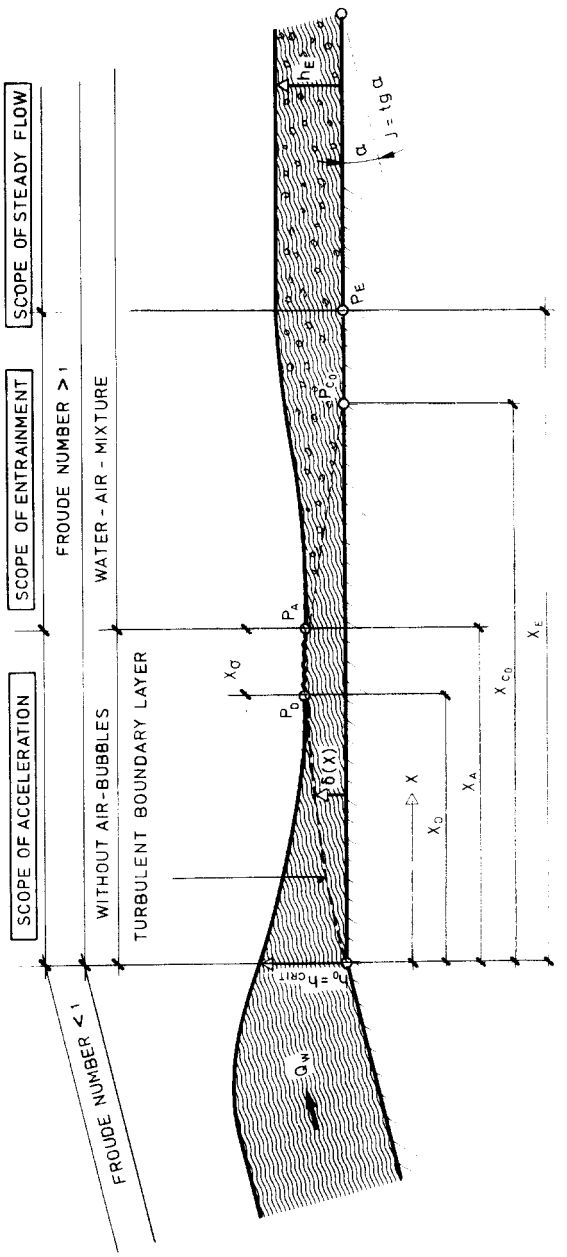

Figure 1. Zones of air-entrainment.

developed for measuring the local air concentration and for the determination of the local velocity of the mixture could be used. They were already extensively described by Gerber (1974), Vischer (1976) and Volkart (1978).

The mentioned instruments made it possible to determine the form, size and motion of particles at the mixture's surface. At the interior of the two-phase flow, the mean size of air bubbles could be reconstructed. But contrary to the drops it was not possible to follow the full course of the bubbles motion.

3. MECHANISM OF THE AIR ENTRAINMENT

The photos in figures 2–6 were the first successfully taken pictures of that kind. They show well perceptible the possible partial processes taking place at the surface of the mixture's flow. The most frequent configuration is the water column, whose length becomes extended due to turbulence and finally slings out one or rarely several water drops. This observation sustains the theory, that slung out water drops, when falling back, drag air bubbles along into the flow's interior. Besides, the surface forms also other shapes, which can be very irregular. More details can be gathered from comments given on the photos. Notice, that on the figures the flow is from right to left!

The systematic interpretation of the pictures brings forth a drop spectrum between 1.0 and 6.5 mm in diameter. Drops, whose dimensions exceed 6.0 mm, quickly lose the spherical shape and decay into separated spherical water particles. This corresponds approximately to Levich (1962), according to whom a free falling water drop reaches in calm air a diameter of 5.2 mm. Therefore it is admissible to assume a spherical shape for the separated water drops.

The observed air bubbles show diameters between 1.0 and 10.0 mm. The size between 2.0 and 7.0 mm appears with a frequency that is greater than average. Also, here exists conformity with the well known diameters of bubbles in open chutes (3.0–8.0 mm).

The answer as to the dominant mechanism of the air bubble entrainement, can be considered the most important result. Air bubbles enter the flow's interior mainly by water drops falling back. Fully developed hydraulic jumps, which entraine air, practically do not exist. The hypothesis about the hydraulic jump presumably derives from the fact that the naked eye

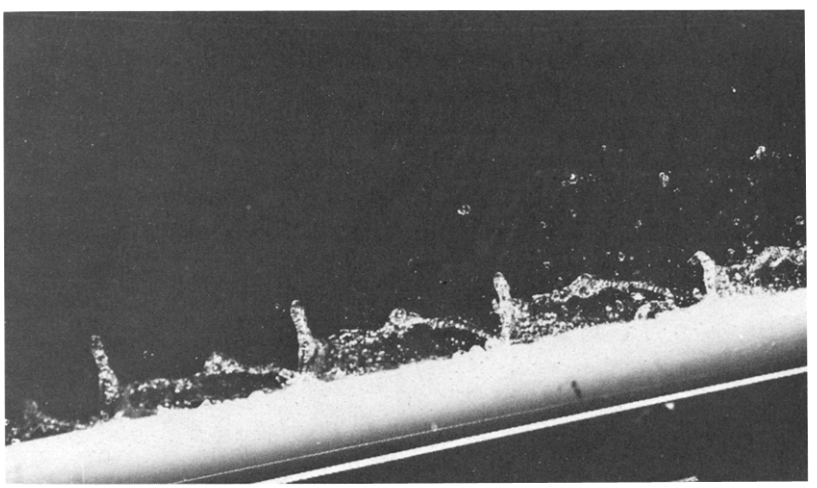

Figure 2. Typical shapes at the mixture surface. A water column is accelerated away from the main flow and slings out a drop of water. When falling back, this drop can drag an air bubble along into the mixture. But also columns can be observed, which have not enough energy as would be necessary to split off some drops. The picture shows a column throwed over the l.h.s., without forming a bubble. Hence, this partial process consumes energy, but does not increase the air concentration.

Here, the flow velocity at the surface is 4.67 m/s and the mean velocity of the total discharge amounts to about the double. The vertically high rising water column is 4 cm high and 5–5.9 mm thick. The perceptible water drop has a diameter of 5.5 mm and is 7.4 cm above the surface.

Figure 3. A characteristic element: the water column stretched upward and slinging out a drop.

cannot follow most of the partial processes going on the mixture's surface. In the studied examples, these processes showed frequencies of 46–56 Hz. By naked eye, one seems to see waves or hydraulic jumps, whereas in reality only many high rised water columns, water drops and air bubbles are simultaneously in motion.

4. MECHANISM OF THE BUBBLE FORMATION: PHYSICAL MODEL, ENERGY CONSIDERATIONS

In addition to the photos, in figure 7 it is shown how a bubble is created from a drop. Several phases can be distinguished:

(a) The water drop strikes the surface in an approximately perpenticular direction.

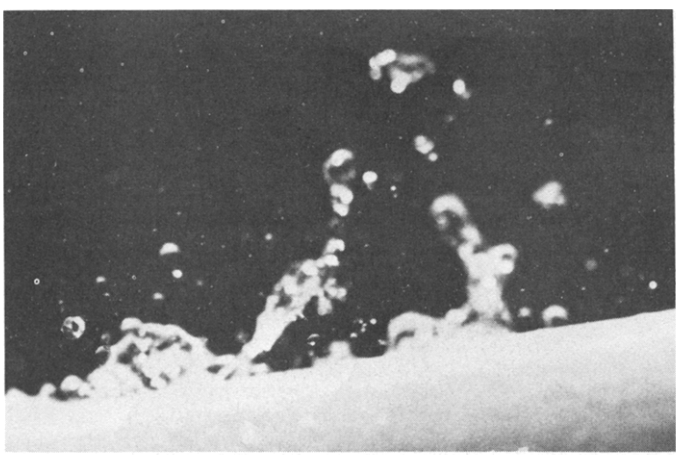

Figure 4. It is perceptible, that at the same spot on the surface, drops can be slinged off into different directions. The velocity component of the drop, which is parallel to the flow direction, does not really have to be identical with the velocity of the discharge at the surface.

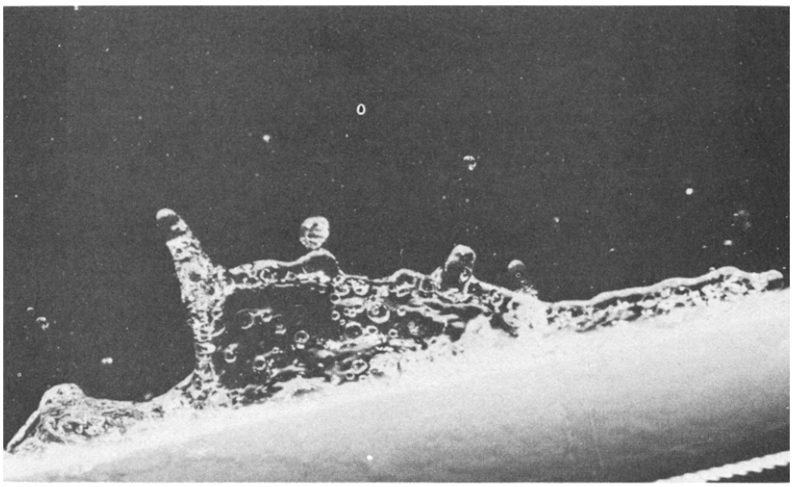

Figure 5. Irregular and symmmetrical shapes, as are shown here, indicate that not only ideal water column-drops can be formed. The free drop in the middle of the picture has a diameter of 5.6 mm. The spherical bubbles are 1–5 mm large.

(b) After the drop hits the surface it becomes partially flattened out. Simultaneously, a water crater is formed.

(c) The drop is slowed down to an unknown depth; a water ring is formed.

(d) Under the influence of the surface tension, the mentioned ring begins to close.

(e) When the lamina is completely closed a bubble has been produced. It is now exposed to the following influences: our remaining impulse, surface tension (shape stability), buoyancy, flow pressure with turbulent fluctuations, thermal and chemical concentration differences (mass transport through the drop interface).

Figure 8 shows the situations, as they can be assumed for an energy consideration. We shall relate the size of a drop and that of the resulting bubble, and determine the minimum fall velocity of that drop, which is necessary to form the bubble. Furthermore, it shall be estimated how high a drop must be slinged out, in order to reach the said unknown velocity whilst falling back.

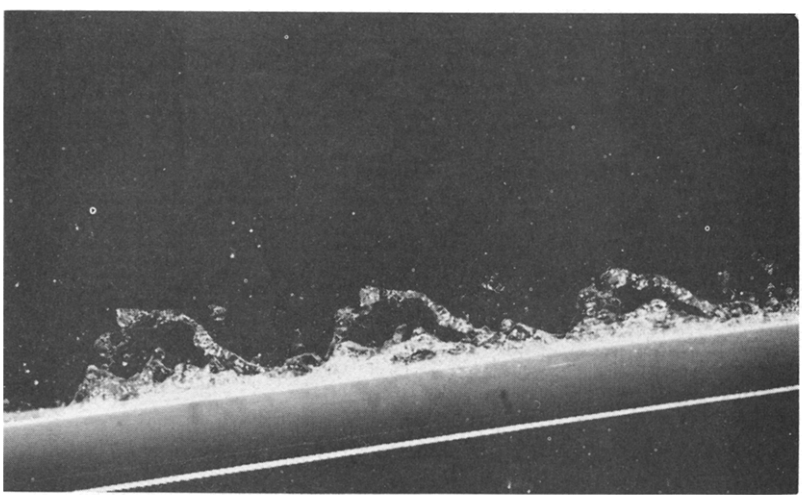

Figure 6. Small hydraulic jumps, which turn over rapidly, seldom entrain air into the water. But for the human eye, they look like vortices with horizontal axes. The stroboscope's frequency for this picture was about 54.2 Hz. Exposure time was 1/10 sec.

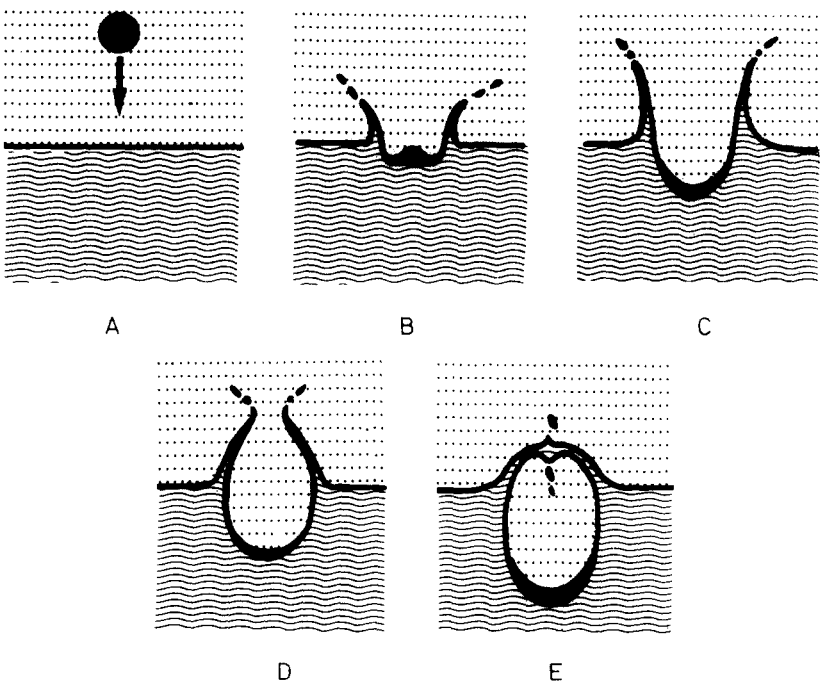

Figure 7. Formation of an air-bubble by a falling water-drop.

Two situations are considered: In situation I, the drop with the diameter D_d and the velocity v_1 is just hitting the water surface. In situation II, the bubble has just formed. It still is dominated by atmospheric pressure. The following symbols are used:

D_d	drop diameter
ρw	mass density of water
m_d	mass of the drop
v_1	velocity of a drop when reaching the water surface
EK_1	kinetic energy of the drop when reaching the water surface
EP_1	potential energy of the drop when reaching the water surface
ES	energy of a drop necessary to overcome the surface tension of the water surface
T	absolute temperature
g	gravitional acceleration

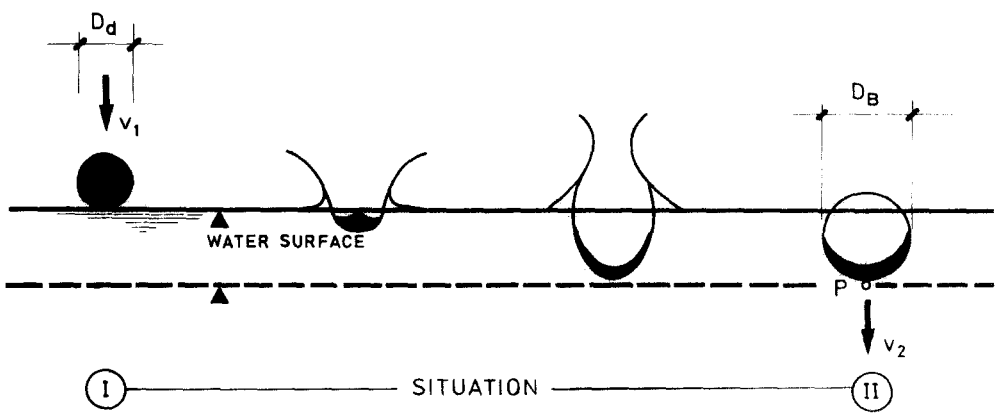

Figure 8.

σ surface tension water–air
C_T coefficient by Witte (1965) = 0.0001425 N/m K
D_B bubble diameter
ρa mass density of air
m_B mass of the bubble
v_2 velocity of a drop + bubble at the moment of the bubble formation
A retarding factor = $1-(v_2/v_1)$
EK_2 kinetic energy of a drop + bubble at the moment of the bubble formation
EP_2 potential energy of a drop + bubble at the moment of the bubble formation.

In situation I, immediately before the drop's contact with the water level, the following formulae are valid:

$$EK_1 = (1/2) \times m_d \times v_1^2$$
$$= (\pi/12) \times \rho w \times v_1^2 \times D_d^3 \quad [1]$$
$$EP_1 = m_d \times g \times (D_d/2 + D_B/2)$$
$$= (\pi/12) \times g \times \rho w \times D_d^3 \times (D_d + D_B) \quad [2]$$

where the zero level of potential energy is $D_B/2$ below the surface. According to Witte (1969), the energy necessary to overcome the surface tension of the water amounts to:

$$ES = \pi \times (\sigma + T \times C_T) \times (D_B^2 - D_d^2). \quad [3]$$

In situation II, immediately after the moment of the bubble formation, the following formulae are valid:

$$EK_2 = (\pi/12) \times v_2^2 \times (\rho w \times D_d^3 + \rho a \times D_B^3) \quad [4]$$
$$EP_2 = (\pi/12) \times g \times \rho a \times D_B^4 \quad [5]$$

where it has been assumed, that the mass of the deformed drop is concentrated in point P on the zero level of potential energy. Heat transport and mass exchange have been neglected. Assuming that the viscous energy which is dissipated between the time of drop impact and the time of cavity closure is small enough to be neglected, the energy balance can now be written down:

$$EK_1 + EP_1 - ES - EK_2 - EP_2 = 0. \quad [6]$$

In combination with [1]–[5] results an equation of the fourth order for the bubble diameter D_B:

$$D_B^4(g \times \rho a) + D_B^3(\rho a \times v_1^2(1-A)^2) + D_B^2(12(\sigma + T \times C_T)) - D_B(g \times \rho w \times D_d^3)$$
$$+ \rho w(v_1^2 \times A(A-2) - g \times D_d) \times D_d^3 - 12(\sigma + T \times C_T) \times D_d^2 = 0. \quad [7]$$

Now, we still have to find characteristic values for the drop diameter D_d, the drop velocity v_1 and the retarding factor A. Nevertheless, the fundamental relation described by [7] can be plotted for assumed realistic parameters D_d and A (figure 9).

It shows that with increasing velocity and size of the drop, the formed bubble's diameter grows. Greater retarding factor A during the drop formation corresponds to greater bubbles. In practice, the bubble's diameter is always greater than the diameter of the generating drop.

Now, if the numerical values of the energies EK_1, EP_1, EK_2 and EP_2 are calculated, it can

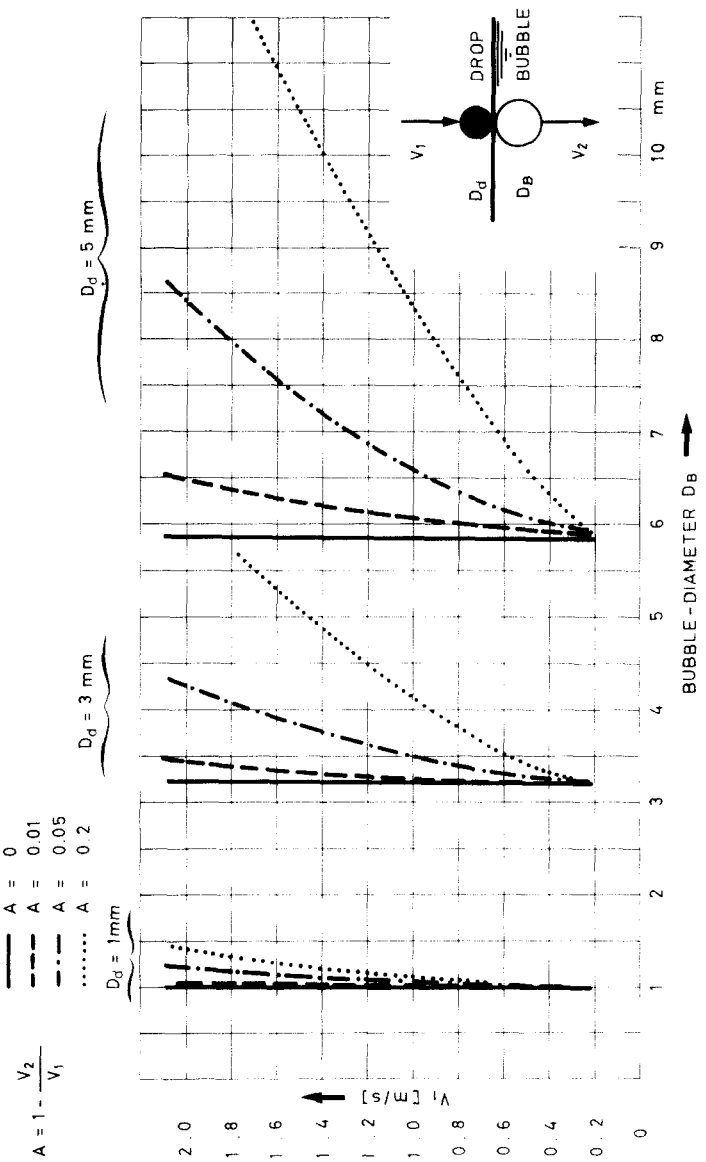
A = 1 - V2/V1
A = 0
A = 0.01
A = 0.05
A = 0.2
Dd = 1mm
Dd = 3 mm
Dd = 5 mm
V1 [m/s]
BUBBLE-DIAMETER DB
DROP
BUBBLE
V1
V2
Dd
DB
mm

Figure 9.

be noticed that the potential energies are at least a hundred times smaller than the other ones. Therefore, it is permissible to simplify the energy balance as follows;

$$ES = EK_1 - EK_2. \qquad [8]$$

Assuming that $\rho a \ll \rho w$, we achieve accordingly for the retarding A:

$$A = 1 - \sqrt{\left(1 - \frac{ES}{EK_1}\right)}. \qquad [9]$$

This last equation still contains implicitly the unknown values D_B and A. Therewith it complies with the fact that from several drops with equal values D_d and v_1 either small bubbles with a small A (profound immersion into the water) or big bubbles with a big A (insignificant immersion) can be formed. It is a statistical phenomenon. Based on the measurements carried out, it is possible to give more concrete information.

5. MINIMUM VELOCITY NECESSARY TO FORM A BUBBLE

The minimum striking velocity of a drop, necessary to form a bubble, can be found considering that the velocity v_2 is zero immediately after the bubble formation. Hence, the kinetical energy EK_2 will also be zero. In this marginal condition we have:

$$\pi \times (\sigma + T \times C_T)(B^2 - 1)D_d^2 = \frac{\pi}{12} \times \rho w \times v_1^2 \times D_d^3 \qquad [10]$$

with $B = D_B/D_d$. Thereof results

$$v_{1\min} = \sqrt{\left[\frac{12}{\rho w \times D_d}(\sigma + T \times C_T)(B^2 - 1)\right]}. \qquad [11]$$

The measurements have brought forth that $1.0 \leq B \leq 1.6$. This permits the presentation of the following table. The values for $v_{1\min}$ fluctuate between 0.2 and 1.5 m/s.

Table 6.

D_d mm	$B = D_B/D_d$	$v_{1\min}$ m/s
1		0.53
3	1.10	0.31
5		0.24
1		1.06
3	1.35	0.61
5		0.47
1		1.46
3	1.60	0.84
5		0.65

6. MINIMUM HEIGHT OF FALL OF A DROP ($H_{\min}$), NECESSARY TO FORM A BUBBLE

For constructive reasons, it is interesting to know the vertical height of fall $H_{\min}$ of a drop which, when striking the flow surface, will just have the velocity $v_{1\min}$. Assuming that the drop

is spherical, then the differential equation for the motion of a falling sphere must be solved. The following terms are valid:

$$\cosh(x) = \frac{e^x + e^{-x}}{2}$$

$$\text{Artanh}(x) = \frac{1}{2} \ln \frac{1+x}{1-x}.$$

m_d = mass of the drop; h_d = distance from the culmination point on; v_d = instantaneous velocity; W_d = air resistance = $\pi \times \frac{D_d^2}{4} \times \frac{\rho a}{2} \times v_d^2 \times \xi_d = C_d \times v_d^2$; and t = time. (For the seldom-appearing drops of big size, W_d will be a little bit smaller.)

The differential equation for the motion is:

$$m_d \times g - W_d = m_d \times \frac{d^2 h_d}{dt^2} = m_d \times \ddot{h}_d. \qquad [12]$$

With the initial conditions

$$h_d(t=0) = \dot{h}_d(t=0) = \ddot{h}_d(t=0) = 0. \qquad [13]$$

By taking:

$$\sqrt{\left(\frac{m_d \times g}{C_d}\right)} = \mu \qquad [14]$$

and integrating it twice for the time t, the result will be:

$$\frac{\mu^2}{g} \times \ln\left(\cosh\left(\frac{g}{\mu} \times t\right)\right) = h_d. \qquad [15]$$

If the expressions for μ and $v_{1\min}$ are assigned, the formula for the minimum height of fall will finally be:

$$H_{\min} = \frac{4}{3} \times \frac{\rho w \times D_d}{\rho a \times \xi_d} \times \ln\left[\cosh\left\{\text{Artanh}\left(\frac{3}{\rho w \times D_d} \times \sqrt{\left(\frac{\rho a \times \xi_d(\sigma + T \times C_T)(B-1)}{g}\right)}\right)\right\}\right]. \qquad [16]$$

This equation is evaluated in figure 10. The ranges for the drop diameter D_d and for $B = D_B/D_d$ were taken from the measurements which were carried out. The range, which in the results could be verified with measured data, is drawn in shaded style. It is unmistakable, that already a height of fall of only a few centimeters can be enough to form bubbles and to increase the air concentration in a two-phase flow.

Using the energy equation [7] or [11] and [16] it is not possible to compute the mean air bubble concentration C of spillway or pipe flow. A water drop dragging bubbles into the two-phase flow has slung out of the flow's surface because of the local turbulent momentum. So, the air entrainment depends on the laws of statistics and the retarding factor A is not exactly determinable. For that reason it is impossible to know how many drops are generating bubbles at a certain moment. In general, the momentary kinetic energy of a drop cannot be predicted from the initial and boundary conditions of the high velocity flow.

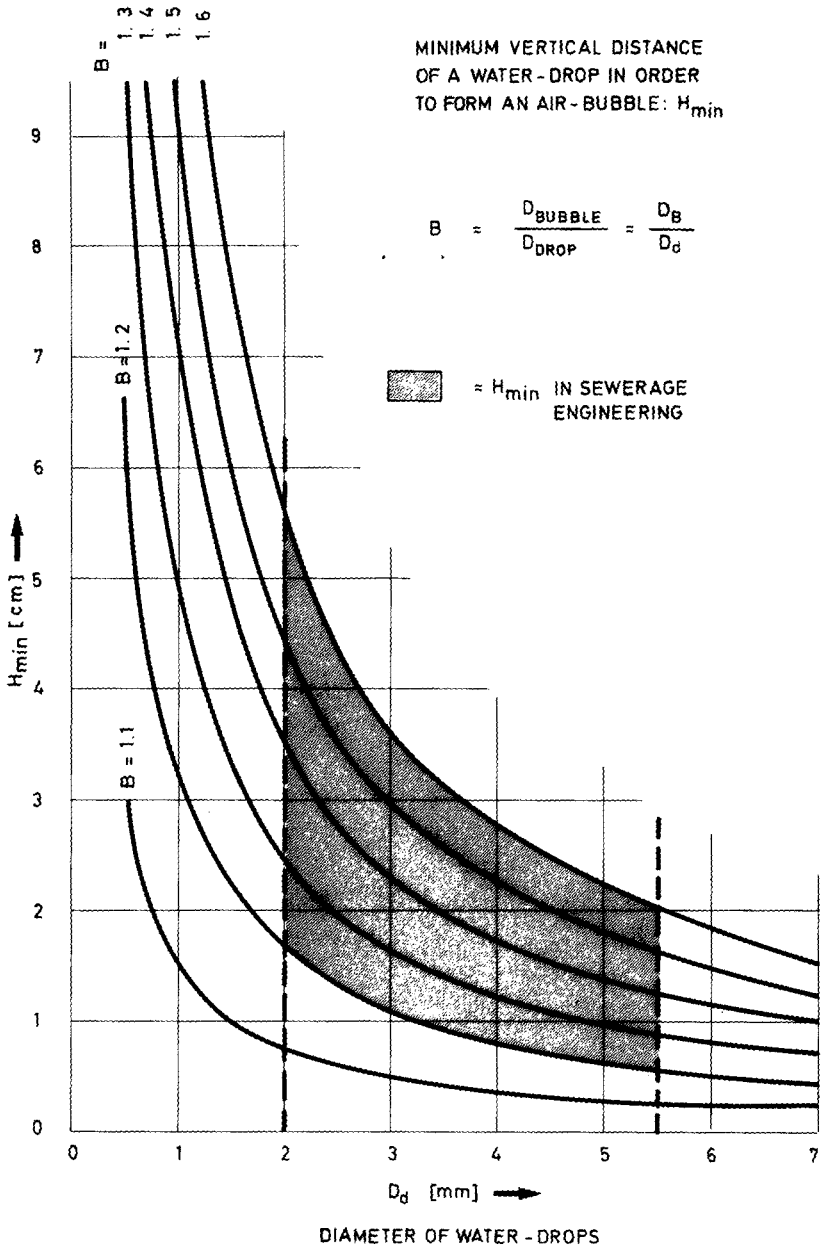

Figure 10. Minimum vertical distance of a water-drop in order to form an air-bubble: H_{min}.

7. CONCLUSIONS

The following conclusions can be summarized as:

—With the stroboscope technique, it is possible to make visible the process of the air bubble entrainement at the surface of quick flowing water.

—In chutes, spillways, steep and partially filled pipelines, air bubbles appear in the water, mainly by slinged off and falling back water particles.

—The drops form out of water columns which have a somewhat thickened "head". Their length becomes stretched and drops separate due to the turbulent transverse pulse of the two-phased flow.

—Beside water columns there exist also other irregular shapes. They also change their shape very quickly, but seldom form any air bubbles. Therefore, these configurations transform flow energy without increasing the air concentration.

—The stroboscope has the capacity to distinguish partial processes, which for the human eye are not more detectable. What the eye recognizes as hydraulic jumps and vortices, are in reality quick moving single water columns, etc.

—The produced bubbles increase in size as diameter and velocity of the pertinent drops increase.

—A bubble is always larger than the pertinent drop. The ratio is: $1 \leq D_B/D_d \leq 1.6$.

—Drop diameters of 1–6 mm were observed. Drops larger than 6 mm lose rapidly the spherical shape and become parted.

—The measured bubble diameters had about 1–10 mm.

—The bursting and fusing of single bubbles could not be made visible with the utilized measuring device.

—The minimum velocity and height of fall of a drop, which is needed to form a bubble, can be calculated ([11] and [16]). There is a good conformity with the measurements.

—The minimum height of fall a drop needs to form a bubble is only a few centimeters ([16], figure 10). For large drops this height of fall is smaller than for small drops.

—Bubbles near the surface are in average larger than those in greater depths. This not only because of the statistical influence due to pressure and bouyancy but also because of the formation mechanism.

—The curved cover in a partially filled pipe exerts an attenuating influence over the air entrainment process. Drops hit on the walls and are slowed down and thus cannot form bubbles so easily. With equal flow coefficients, the mean air concentration in an open channel is therefore greater than in a partially filled pipeline.

—The measuring results are valid for clean water and slightly dirty sewage water.

As already mentioned, the mean air concentration C cannot be calculated from [1]–[16]. In general one tries to correlate the measured values of C with the usual dimensionless numbers as the Froude number Fr, the Reynolds number Re or the Weber number We.

But doing that the mechanism of air bubble entrainment by water drops has really not taken into account. Besides, in a water–air-mixture both, the kinematic viscosity γ (for Re) and the surface tension σ (for We) are function of the concentration C too.

For two-phase flows in inclined partially filled pipes the author was able to propose such an empirical equation including the Boussinesq number which corresponds very well with the measured data (Volkart 1978).

REFERENCES

Bauer, W. 1954 Turbulent boundary layer on steep slopes. *ASCE Trans.* **2719**, 1212–1242.

Ehrenberger, H. 1926 Wasserbewegungen in steilen Rinnen. *Mtg. Wien* **6**, Folge.

Frankovic, A. 1953 Head loss and air entrainment by flowing water in steep chutes. Proc. IAHR 467–476.

Gerber, U. 1974 Velocity measurement of water–air mixtures. Exp. IWRA, Chicago, June.

Hickox, H. 1945 Air entrainment on spillway faces. *Civil Engng* 562–563.

Keller & Rastogi, 1975 The prediction of flow development on Spillways. *J. Hydr. Div.* 1371–1404.

Killen & Anderson 1969 A study of the air-water interface in air-entrained flow in open channels. 130 IAHR Cong., Subj. B36.

Lane, E. 1939 Entrainment of air in swiftly flowing water. *Civil Engng* 89–91.

Siemens, W. 1954 Gasblasen in Flüssigkeiten. *Chem. Ing. Techn.* **11**, 614–630.

Viparelli, M. 1958 Correnti rapide. *Energia Elettrica* 7, 633–649.

Vischer, Volkart & Näf 1976 Hydraulische Modellversuche für die Abwassertechnik. *Wasser, Energie, Luft* **2**, 53–62.

VOLKART, P. 1978 Hydraulische Bemessung steiler kanalisationsleitungen unter Berücksichtigung der Luftaufnahme. Diss. ETH Zürich 6104.

VOLKART, P. 1978 Hydraulische Bemessung teilgefüllter Steilleitungen. *Gas, Wasser, Abwasser* **11**, 658–667.

WITTE, J. 1969 Mixing shocks in two-phase flow. *J. Fluid Mech.* **36**, 639–655.